

Methane Catalytic Combustion on Pd₉/γ-Al₂O₃ with Different Degrees of Pd Oxidation

Izabela Czekaj^{§*}, Katarzyna A. Kacprzak, and John Mantzaras

[§]SCS-DSM Award for best poster presentation

Abstract: This research is focused on the analysis of adsorbed CH₄ intermediates at oxidized Pd₉ nanoparticles supported on γ-alumina. From first-principle density functional theory (DFT) calculations, several configurations, charge transfer and electronic density of states have been analyzed in order to determine feasible paths for the oxidation process. Furthermore methane oxidation cycles have been investigated on Pd nanoparticles with different degrees of oxidation. In case of low oxidized Pd nanoparticles, activation of methane is observed, whereby hydrogen from methane is adsorbed at one oxygen atom. This reaction is exothermic. In a subsequent step, two water molecules desorb. Additionally, a very interesting structural effect becomes evident; Pd-carbide formation, which is also an exothermic reaction. Furthermore, oxidation of such carbided Pd-nanoparticles leads to CO₂ formation, which is an endothermic reaction. One important result is that the support is involved in the CO₂ formation. A different mechanism of methane oxidation was discovered for highly oxidized Pd nanoparticles. When the Pd nanoparticle is more strongly exposed to oxidative conditions, adsorption of methane is also possible, but it leads to carbonic acid production at the interface between the Pd nanoparticles and support. This process is endothermic.

Keywords: Alumina support · DFT · Metal-support interactions · Methane combustion · Palladium catalyst

1. Introduction

In recent years, catalytic combustion of methane over Pd-based catalysts has been widely investigated both experimentally and theoretically. Palladium exhibits the highest catalytic activity for the total oxidation of methane, with PdO being the main active phase under lean combustion conditions.^[1–6] Catalytic activity is strongly influenced by the combustion temperature and the oxygen partial pressure.^[7–10] Palladium exhibits an unusual behavior in both the metallic and oxide state with respect to the catalytic activity during reaction. Spontaneous reversible transformation between the active PdO and the relatively inactive Pd component is correlated with the capacity of temperature self-control, which in turn prevents catalyst sintering.^[1] The catalytic characteristics of palladium are often compared to those of platinum since the latter is more resistant to the presence of sulfur-containing pollutants, even though its performance and stability is worse. A palladium catalyst

provides greater performance for catalytic combustion in boilers and natural-gas-fired turbines, and higher activity towards CO and CH₄ oxidation.^[11]

A kinetic model for oxidation/reduction cycles has been suggested by Wolf *et al.*^[10] A recent study reported that, at O₂ partial pressures corresponding to 2 atm of air, the region of non-monotonic change in activation energy for CH₄ oxidation was absent and the drop of activity was monotonic with decreasing temperature.^[2] Higher O₂ partial pressures restore PdO at sufficiently high temperatures, whereby even the reduced Pd is active for CH₄ oxidation.^[2] Understanding the Pd/PdO behavior at high pressures is critical for catalytic combustion models of practical power generation devices, and care must be exercised when extrapolating low-pressure kinetics to elevated pressures. In addition, the effect of the support on catalytic activity must be well-characterized or minimized in microreactor studies. It has been suggested that the support plays a role in the oxidation and reduction of Pd/PdO particles.^[1] Efforts to develop surface chemistry models for Pd-catalyzed CH₄ oxidation should therefore also include support effects. However, modeling the effect of the support in a surface chemical reaction mechanism is challenging due to the large active nanoparticle sizes. It is further evi-

dent that such a mechanism should include the description of sub-surface processes in the catalyst particles.

Driven by the aforementioned key questions, we have recently investigated by means of density functional theory (DFT) the Pd and PdO defect system,^[12] to address kinetic hypotheses regarding the role of oxygen vacancies in the hysteretic Pd/PdO behavior. It was shown^[12] that Pd and PdO exhibit complex behavior and that the calculated energy of a single surface oxygen vacancy was about 1.3 eV. In the experiments presented by Wolf *et al.*,^[10] Al₂O₃ support was used. DFT modeling of Ni particles supported on a (100) Al₂O₃ surface was carried out previously in our laboratory, yielding promising results regarding the particle deposition behavior that were further verified experimentally.^[13] Oxidation by a single O₂ molecule of different clusters supported on an alumina/NiAl(110) surface has been reported by Robles and Khanna.^[14] We herein consider that support effects should not be neglected in the Pd system. More recently, we investigated the full oxidation of Pd to PdO by comparing both molecular and dissociative adsorption of 1–4 oxygen molecules.^[15]

The main goal of our recent studies was to understand the methane combustion mechanism over Pd-nanoparticles of different degrees of oxidation supported

*Correspondence: Dr. I. Czekaj
General Energy Department
Paul Scherrer Institute
CH-5232 Villigen PSI
Tel.: +41 56 310 44 64
E-mail: izabela.czekaj@psi.ch

on $\gamma\text{-Al}_2\text{O}_3$. Herein, we report the reaction energetics over Pd/alumina with the main objectives to establish a complete methane oxidation cycle and to quantify changes in catalytic activity upon formation of palladium oxide and carbide. Analysis of two different oxidative conditions is undertaken, oxygen-rich and oxygen-deficient.

2. Computational Details

Ab initio calculations within the density functional theory are used in a real space grid implementation of the projector augmented wave (PAW) method using GPAW software.^[16,17] The exchange and correlation functional is approximated with a scalar-relativistic spin-paired Perdew-Burke-Ernzerhof (PBE) formula.^[18] Electrons treated in the valence shell for the different elements are H(1s), O(2s2p6), Al(3s23p1), Pd(3d24s24p6). The grid spacing is set to 0.18 Å in all calculations, which ensures converged energy differences. The structures are relaxed with the quasi-Newton method and regarded as structurally optimized when the largest element of the gradient becomes less than 0.05 eV/Å. The electronic density of states (EDOS) was obtained by a 0.02 eV Gaussian broadening of the one-electron Kohn-Sham energy levels.

3. Results

The cluster-stabilized model for the Pd₉ cluster on a γ -alumina support and the structure of the bare Pd₉ cluster are first introduced. Subsequently, the most stable oxidized Pd₉ nanoparticle is discussed. Finally, the adsorption and oxidation of methane at Pd₉ clusters with different degrees of oxidation is addressed, with further analysis on the electronic structure of each step.

3.1 Modeling of Pd Nanoparticle and γ -Alumina Support

The computational model of Pd₉ nanoparticles on a γ -alumina support is shown in Fig. 1. The model of the support was designed by cropping the bulk of Al₂O₃ and then saturating all surface O atoms (except those in the (100) surface) by hydrogen, in order to maintain the coordination environment and oxidation states of Al₂O₃ in the bulk. Several clusters, which represent Al₂O₃ (100), have been analyzed,^[15] and finally the $\gamma\text{-Al}_{64}\text{O}_{142}\text{H}_{92}$ cluster was used in CH₄ adsorption studies.

3.2 Oxidation of Pd₉ Clusters Supported on γ -Alumina

Several oxidation steps of the Pd₉ cluster supported on alumina were investigat-

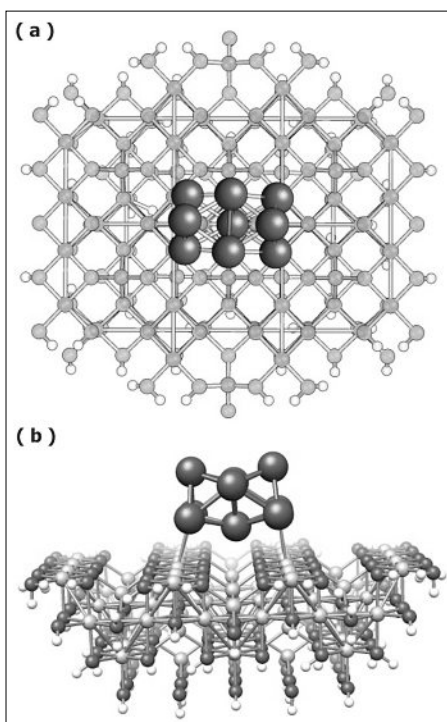


Fig. 1. Structure of the Pd₉ cluster at support (Al₆₄O₁₄₂H₉₂): a) top view b) side view.

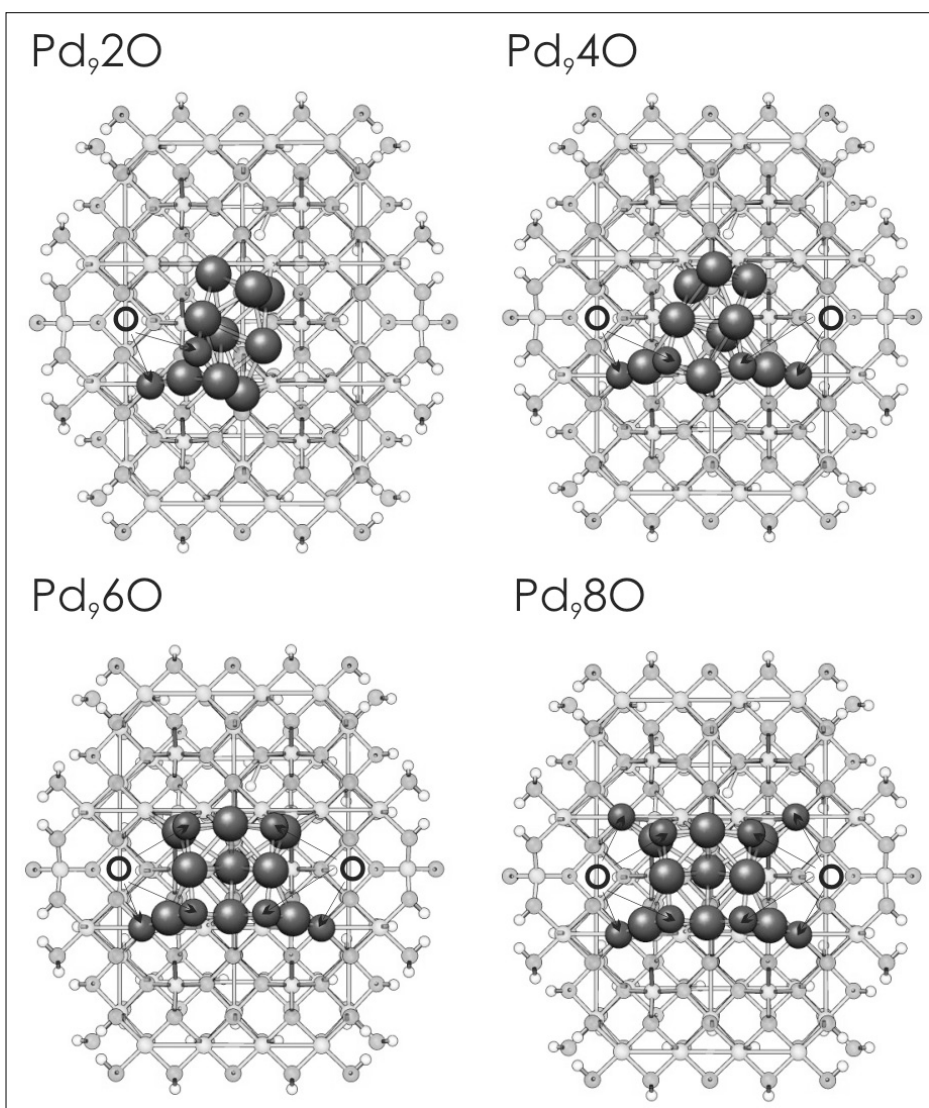


Fig. 2. Oxidation of Pd₉/Al₂O₃ – structure and adsorption sites.

ed, considering one to four molecules of oxygen. Fig. 2 illustrates the structure and adsorption sites for four Pd clusters with different levels of oxidation simulating oxygen-deficient conditions (Pd₉2O), to oxygen-rich conditions with Pd₉ nanoparticles partially oxidized (Pd₉4O and Pd₉6O) up to a fully oxidized Pd cluster (Pd₉8O). Oxidation of Pd₉ is attained by immediate dissociation after adsorption of each oxygen molecule.^[15] The most energetically preferable sites for adsorption are close to the contact between the cluster and the support, where one oxygen atom interacts with 5-coordinated aluminum atoms, and the remaining oxygen is in contact with the closest palladium atom. After first dissociation, one oxygen atom creates a bridge between the palladium and the 5-coordinated aluminum atom and the second oxygen atom moves to the top of the Pd₉ cluster, making a bridge between two palladium centers (see Fig. 2, structure Pd₉2O). The next dissociations arise analogously, with the difference that oxygen atoms in the second layer of the palla-

dium cluster occupy the hollow sides of the cluster. Additionally, the Pd nanoparticle geometry drastically changes (see Fig. 2, Pd₉4O geometry). Such extreme changes in the Pd₉ nanoparticle during oxidation justify two conjectures for the complicated behavior of Pd nanoparticles during the catalytic reaction. First is that the support determines the initial oxidation steps of the metal particle. Second, the dynamics of nanoparticle structural change in each oxidation step would strongly influence further reactivity of Pd nanoparticles, e.g. oxidation of methane under different conditions.

After analyzing the oxidation process of Pd-nanoparticles, it is suggested that different oxidation levels of nanoparticles can lead to different methane oxidation paths due to different location and access to the oxygen.

3.3 Oxidation of Methane on a Pd/Al₂O₃ Catalyst

The HOMO level of the methane molecule is located very deep in the energy range of the nanoparticle valence band ($E = -9.5$ eV) and thus activation proceeds via C-H bond break and formation of CH₃. Therefore CH₃⁺ would be formed on the Pd nanoparticle with a singly occupied molecular orbital (SOMO) energy level that are a better fit to the valence levels of the particle. The advantage of oxidized Pd-particles comes from the lower valence band (compared with Pd-metallic nanoparticles) as well as the presence of surface oxygen. In such conditions CH₃⁺ species can form methoxy groups and lead to the further oxidation of methane.

The methane oxidation cycles have been considered as a further step on Pd nanoparticles with different oxidation levels: i) in oxygen-deficient conditions, ii) in oxygen-rich conditions.

In oxygen deficient conditions, where low oxidation levels of Pd nanoparticles are observed (see Fig. 3, left cycle): As a first step, activation of methane is observed, where hydrogen from methane is adsorbed at one oxygen atom of the Pd nanoparticle. This reaction is exothermic with adsorption energy equal to -0.38 eV. In a subsequent step, activation takes place and desorption of two water molecules is observed. Additionally, a very interesting structural effect is evident, which is Pd-carbide formation, which is also an exothermic reaction ($E = -0.65$ eV). Furthermore, oxidation of such a carbided Pd nanoparticle leads to CO₂ formation ($E = -4.71$ eV). Therefore it is apparent that the support is involved in CO₂ formation (see Fig. 3, structure Pd₉-CO₂). The desorption of CO₂ from this position has an energy equal to 3.23 eV.

In oxygen-rich conditions, extensive

oxidation of Pd nanoparticles is evident (see Fig. 3, right cycle): When the Pd nanoparticles are more strongly exposed to oxidative conditions, the result is a stronger oxidation of the metallic cluster (see Fig. 3, Pd₉6O₄ cluster). Adsorption of methane under these oxidation conditions proceeds in a different way due to oxygen deficiency. In a first step, exothermic first activation of methane is observed above the Pd center and an OH group is formed at the neighbor oxygen ($E = 0.75$ eV). After a few intervening steps, such as further hydrogen interaction with Pd nanoparticles and water formation, carbonic acid is formed at the interface between Pd nanoparticles and support. Again this process is exothermic with an energy of 1.06 eV. The desorption of carbonic acid is exothermic and completes the methane combustion cycle in oxygen-rich conditions.

In all conditions, combustion of methane proceeds with different mechanisms of CH₄ activation and oxidation. However, in all cases the important influence of alumina support is observed.

4. Conclusions

Theoretical studies of methane oxidation cycles at Pd/Al₂O₃ catalysts show that the mechanism of methane activation and combustion strongly depends on the oxygen supply. Concerning metal nanoparticle oxidation itself, it is shown that the support greatly facilitates oxidation of Pd nanoparticles during the initial steps of the oxidation process by attracting one oxygen atom and creating a bridging interface between the support and nanoparticle.^[15] The second oxygen atom migrates and adsorbs

at the Pd-nanoparticle surface. Further adsorption of oxygen causes strong changes in symmetry and shape of the Pd nanoparticle. However, half of the oxygen atoms are always deposited between the support and the Pd nanoparticle. The dynamics of the structural changes of nanoparticles in each oxidation step strongly influences the further reactivity of Pd nanoparticles. After analyzing the oxidation process of Pd nanoparticles, it is suggested that different oxidation levels of nanoparticles can lead to different methane oxidation paths due to different locations and access to the oxygen in the Pd nanoparticles.^[15] In the case of a low oxidation level of the Pd nanoparticle, activation of methane is observed, where hydrogen is adsorbed at one oxygen atom. Due to the lack of oxygen, Pd₃C is formed and after additional adsorption of oxygen CO₂ is produced. However, when the Pd nanoparticle is more strongly exposed to oxidative conditions, adsorption of methane is also possible, but it will result in carbonic acid production at the interface between Pd nanoparticles and support.

Acknowledgements

Support from the Swiss National Foundation under Project No. 200021-116184/1 is gratefully acknowledged. CPU time has been provided by CSCS (Manno, Switzerland) as well as PSI local cluster.

Received: January 2, 2013

- [1] R. J. Farrauto, M. C. Hobson, T. Kennelly, E. M. Waterman, *Appl. Catal. A: General* **1992**, *81*, 227.
- [2] P. Forzatti, *Catal. Today* **2003**, *83*, 3.
- [3] P. Forzatti, G. Groppi, *Catal. Today* **1999**, *54*, 165.

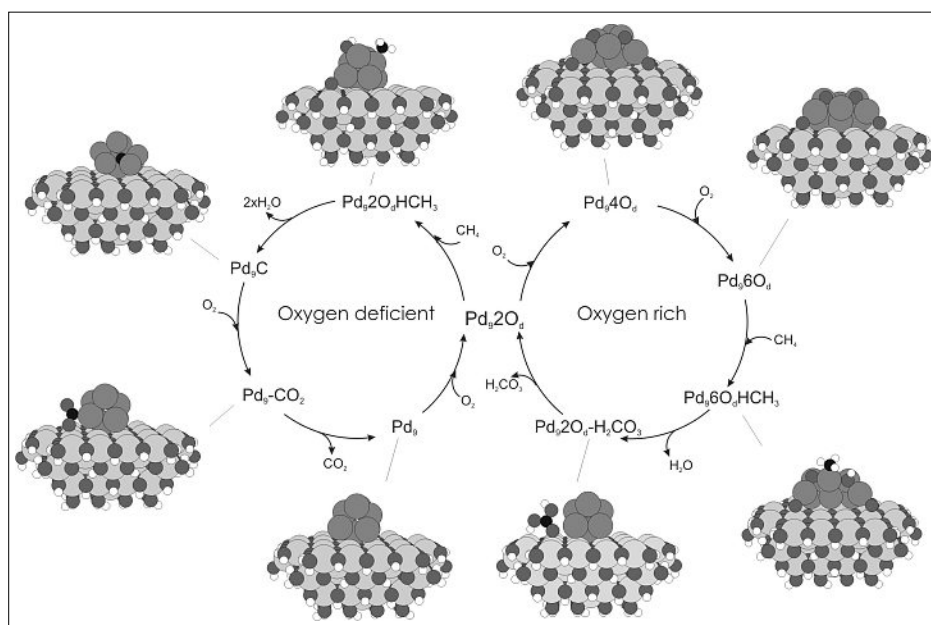


Fig. 3. Oxidation of methane. Two different oxidation cycles: oxygen deficient (left) and oxygen rich (right).

- [4] D. Ciuparu, M. R. Lyubovsky, E. Altman, L. D. Pfefferle, A. Datye, *Catal. Rev.* **2002**, *44*, 593.
- [5] D. Ciuparu, L. Pfefferle, *Appl. Catal. A: General* **2001**, *415*, 209.
- [6] R. Carroni, T. Griffin, J. Mantzaras, M. Reinke, *Catal. Today* **2003**, *83*, 157.
- [7] S. A. S. Reihani, G. S. Jackson, *Proc. Combust. Inst.* **2002**, *29*, 989.
- [8] C. A. Müller, M. Maciejewski, R. A. Koepfel, A. Baiker, *J. Catal.* **1997**, *166*, 36.
- [9] J. Au-Yeung, A. T. Bell, E. Iglesias, *J. Catal.* **1999**, *185*, 213.
- [10] M. W. Wolf, H. Zhu, W. H. Green, G. S. Jackson, *Appl. Catal. A: General* **2003**, *244*, 323.
- [11] O. Deutschmann, R. Schmidt, F. Behrendt, J. Warnatz, *Proc. Combust. Inst.* **1996**, *26*, 1747.
- [12] M. Bruska, I. Czekaj, B. Delley, J. Mantzaras, A. Wokaun, *Phys. Chem. Chem. Phys.* **2011**, *13*, 15947.
- [13] F. Loviat, I. Czekaj, J. Wambach, A. Wokaun, *Surf. Sci.* **2009**, *603*, 2210.
- [14] R. Robles, S. N. Khanna, *Phys. Rev. B* **2010**, *82*, 085428.
- [15] K. Kacprzak, I. Czekaj, J. Mantzaras, *Phys. Chem. Chem. Phys.* **2012**, *14*, 10243.
- [16] J. J. Mortensen, L. B. Hansen, K. W. Jacobson, *Phys. Rev. B* **2005**, *71*, 035109.
- [17] J. Enkovaara, C. Rostgaard, J. J. Mortensen, J. Chen, M. Dulak, L. Ferrighi, J. Gavnholt, C. Glinsvad, V. Haikola, H. A. Hansen, H. H. Kristoffersen, M. Kuisma, A. H. Larsen, L. Lehtovaara, M. Ljungberg, O. Lopez-Acevedo, P. G. Moses, J. Ojanen, T. Olsen, V. Petzold, N. A. Romero, J. Stausholm, M. Strange, G. A. Tritsarlis, M. Vanin, M. Walter, B. Hammer, H. Häkkinen, G. K. H. Madsen, R. M. Nieminen, J. K. Nørskov, M. Puska, T. T. Rantala, J. Schiøtz, K. S. Thygesen, and K. W. Jacobson, *J. Phys.: Condens. Matter* **2010**, *22*, 253202.
- [18] J. P. Perdew, K. Burke, M. Ernzerhof, *Phys. Rev. Lett.* **1996**, *77*, 3865.